Efficient Selection of High-Order Laguerre–Gaussian Modes in a Q-Switched Nd : YAG Laser

Amiel A. Ishaaya, *Student Member, IEEE*, Nir Davidson, Galina Machavariani, Erez Hasman, and Asher A. Friesem, *Fellow, IEEE*

***Abstract*—Intra-cavity binary phase elements are incorporated into a Q-switched Nd : YAG laser resonator to obtain efficient high-order transverse mode selection. The resonator configuration is analyzed using the propagation-matrix diagonalization method and the Fox–Li algorithm, and a simple model for predicting the relative output powers of the selected modes is developed. The predicted results are verified experimentally with binary phase elements for selecting the TEM_{01}, TEM_{02} and TEM_{03}, degenerate Laguerre–Gaussian modes. The output energy per pulse was 15 mJ for the TEM_{01}, 16.5 mJ for TEM_{02} and 18.3 mJ for TEM_{03}, all higher than the 10mJ for the TEM_{00}. The performance in Q-switched operation was found to be similar to that in free-running operation. The numerical calculations, experimental procedure and experimental results are presented.**

***Index Terms*—Beam shaping, laser resonators, mode selection, phase elements, Q-switched lasers, solid-state lasers.**

I. Introduction

THE OUTPUT beam quality emerging from a stable laser resonator that operates with many transverse modes is relatively poor. The beam quality can be improved by inserting an aperture inside the resonator in order to reduce the effective radius of the gain medium until, at best, only the fundamental TEM_{00} mode of the Gaussian shape exists. Unfortunately, the introduction of the aperture results in a significant reduction of the output power, since only a small volume of the gain medium is exploited. In order to increase the output power with respect to the fundamental mode operation, while obtaining a reasonable beam quality, one could operate the laser in a single high-order mode, exploiting a relatively large volume of the gain medium. The beam quality of a single high-order mode beam can be further improved by efficiently transforming it into a nearly Gaussian beam [1]–[3]. In recent years, new methods for operating a laser with a single high-order transverse mode have been reported (see review [1]). These methods are based on the insertion of binary and spiral phase elements within the laser resonator, so as to introduce high losses to the undesired low-order modes and low losses to the desired mode. The undesired high-order modes are eliminated in the conventional way by using an intra-cavity aperture. Efficient high-order mode selection using these methods was demonstrated only in CW lasers, where low gain was present [4], [5].

Manuscript received June 20, 2002; revised September 3, 2002.

A. A. Ishaaya, N. Davidson, G. Machavariani and A. A. Friesem are with the Department of Physics of Complex Systems, Weizmann Institute of Science, Rehovot 76100, Israel (e-mail: feami@wisemail.weizmann.ac.il).

E. Hasman is with the Optical Engineering Laboratory, Faculty of Mechanical Engineering, Technion—Israel Institute of Technology, Haifa, Israel (e-mail: mehasman@tx.technion.ac.il).

Digital Object Identifier 10.1109/JQE.2002.806164

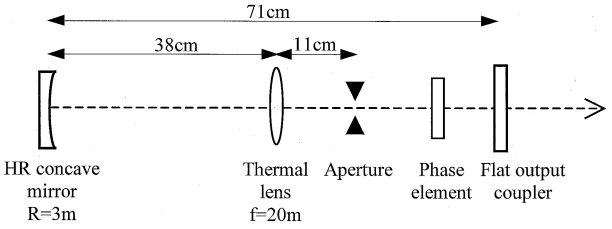

Fig. 1. Simple plano-concave resonator configuration for high-order mode selection.

In this paper, we demonstrate, for the first time, efficient high-order mode selection in a Q-switched (QS) Nd : YAG laser. Specifically, we show that it is possible to overcome the difficulties in selecting a single transverse mode that result from the inherent high gain and complex mode dynamics in such lasers [6], [7], by resorting to intra-cavity binary phase elements. The resonator design, along with mode content analysis and wave simulation predictions are described in Section II. These include numerically solving the round-trip propagation equation, obtaining the mode patterns and associated loss, combined with numerical Fox–Li calculations demonstrating the selection of the high-order modes. A simple model for predicting the relative output energies of the selected modes is presented in Section III. The experimental setup and the experimental results are described in Section IV, and concluding remarks are given in Section V.

II. Resonator Design and Analysis

Let us consider the mode selection in a basic plano-concave resonator configuration depicted in Fig. 1. It consists of a flat output coupler mirror, an internal lens with $f = 20$ m to account for thermal lensing, a high reflective concave back mirror with a curvature radius of 3 m, an aperture to limit the number of high-order modes, and a phase element for mode selection. This configuration was chosen rather than a flat–flat configuration in order to decrease the sensitivity to thermal lensing, and to enhance the mode selectivity of the resonator [8].

We first begin with analyzing the *bare* resonator configuration, not taking into account the gain medium effects (except for a constant thermal lensing). In order to determine the mode content in the resonator, it is necessary to solve the round-trip propagation equation of

$$\boldsymbol{K}\boldsymbol{U}_{\boldsymbol{n}} = \gamma_n \boldsymbol{U}_{\boldsymbol{n}} \tag{1}$$

0018-9197/03$17.00 © 2003 IEEE

where the eigenvectors $\boldsymbol{U_n}$ represent the field distribution of the resonator modes, $\boldsymbol{K}$ represents the round-trip propagation kernel, and the power loss per round-trip $1-|\gamma_n|^2$ is obtained from the eigenvalues γ_n. Equation (1) can be solved numerically by using the propagation-matrix diagonalization method [1]. In this method, each optical element in the resonator and the free-space field propagation, are represented by matrix operators. The round-trip matrix $\boldsymbol{K}$ is found by multiplying all the matrix operators associated with the round trip, and then the eigenfunctions and eigenvalues are obtained by diagonalizing $\boldsymbol{K}$. In order to reduce the calculation complexity, we assume radial symmetry, so the eigen solutions for each mode of radial order p and azimuthal order l can be written as

$$U_{p,l}(r,\,\phi,\,z) = U_{p,l}(r,\,z)\exp(il\phi) \tag{2}$$

where r is the radial coordinate, ϕ is the azimuthal coordinate, and z is the position along the propagation direction.

With radial symmetry, the eigenvector $\boldsymbol{U_n}$ represents the radial field of the mode at the output coupler, and the round trip matrix K takes the form of

$$\boldsymbol{K} = \mathrm{M_{FS}}\cdot\mathrm{M}_{AP}\cdot\mathrm{M_{FS}}\cdot\mathrm{M}_{L}\cdot\mathrm{M_{FS}}\cdot\mathrm{M_{RM}}\cdot\mathrm{M_{FS}}\cdot\mathrm{M}_{L} \cdot\mathrm{M_{FS}}\cdot\mathrm{M}_{AP}\cdot\mathrm{M_{FS}} \tag{3}$$

where $\mathrm{M_{FS}}$ is the free-space propagation matrix, $\mathrm{M_{AP}}$ is the aperture matrix, M_L is the thermal lensing matrix, and $\mathrm{M_{RM}}$ is the rear concave mirror matrix (all 2-D matrices). The propagation matrix $\mathrm{M_{FS}}$ for each azimuthal order l could be determined from the radial Kirchhoff–Fresnel diffraction kernel for long distances [9], given by

$$U_l(r_2,\,z_0) = i^{l+1}kz_0^{-1}\exp(-ikz_0)\int U_l(r_1,\,0)J_l(kr_1r_2/z_0) \cdot\exp[-ik(r_1^2+r_2^2)]r_1\,dr_1 \tag{4}$$

where z_0 is the propagation distance, k=$2\pi/\lambda$, and r_1 and r_2 are the radial coordinates at $z=0$ and $z=z_0$, respectively. Alternatively, $\mathrm{M_{FS}}$ could equally be determined from the angular spectrum propagation for short distances [10].

We calculated the low-order eigenvectors and their corresponding losses for the resonator configuration shown in Fig. 1, without the phase element and for $\lambda = 1064$ nm. The results are presented in Figs. 2 and 3. Fig. 2 shows the losses as a function of the intra-cavity aperture diameter, and Fig. 3 shows the radial intensity distributions of the lowest order modes for two specific aperture diameters. It can be seen that as the aperture radius increases (larger Fresnel number; $N_F = a^2/\lambda L$, where a is the aperture radius, λ is the wavelength and L is the resonator length) the losses of all modes decrease, and multimode operation is expected. In order to select the lowest order mode, one usually closes the aperture until only the lowest order mode could exist (depending on the gain). The intensity patterns depicted in Fig. 3 closely resemble the nondegenerate Laguerre–Gaussian (LG) modes, as expected with radial symmetry. However, it should be noted that these are not exact LG modes, since the field diffraction

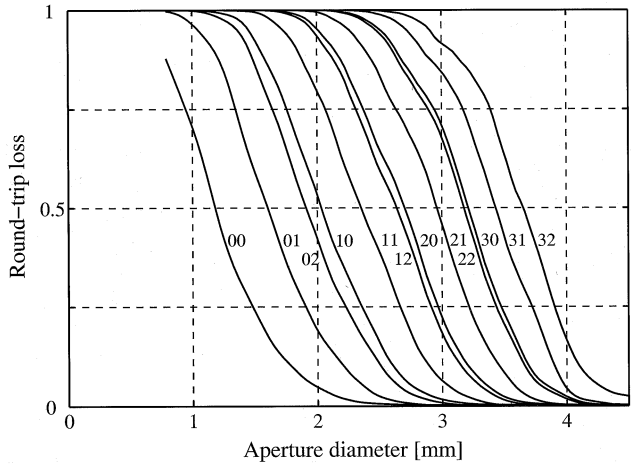

Fig. 2. Calculated round-trip losses of the lowest order modes as a function of intra-cavity aperture diameter for the *bare* resonator configuration without a phase element. Based on numerical matrix diagonalization in radial symmetry.

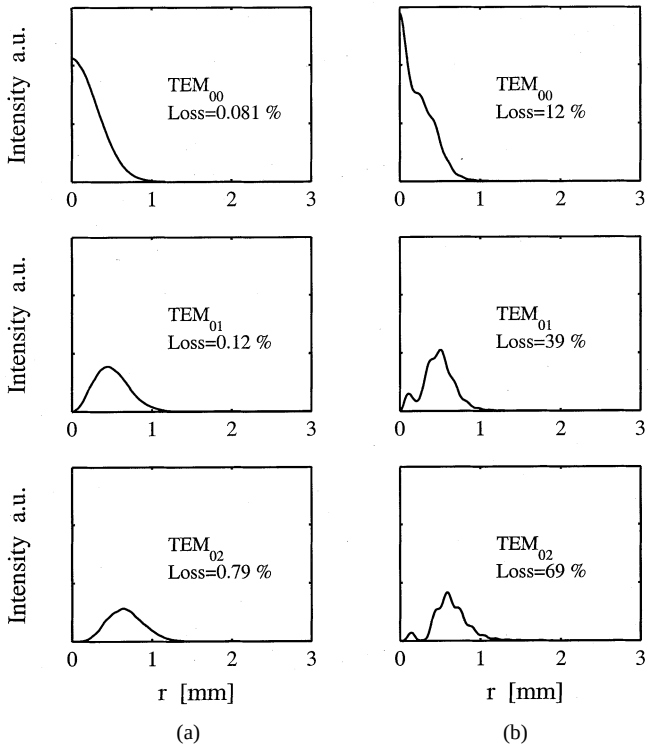

Fig. 3. Calculated intensity distributions of the lowest order modes for the *bare* resonator configuration without a phase element. (a) Aperture diameter -3 mm. (b) Aperture diameter -1.7 mm.

losses at the aperture affects the modes distributions. Indeed, at small aperture diameters, the modes intensity distributions are expected to significantly differ from the LG modes.

In order to obtain single high-order mode operation, a phase element is introduced into the resonator, next to the output coupler (see Fig. 1). This element introduces high losses to the undesired low order modes, and low losses to the desired high-order mode. Very high-order modes are eliminated by the use of the aperture. We investigated the effect of three different binary phase elements for selecting the $\mathrm{TEM_{01}}$, $\mathrm{TEM_{02}}$, and $\mathrm{TEM_{03}}$ degenerate LG modes. These elements, shown schematically in Fig. 4, consist of π phase steps, corresponding to the uniform

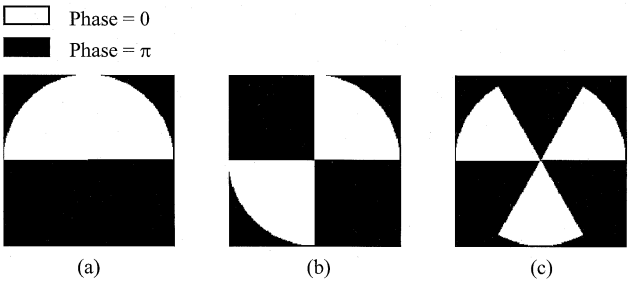

Fig. 4. Phase distribution of the binary phase elements for selecting the degenerate LG modes: (a) TEM_{01}; (b) TEM_{02}; and (c) TEM_{03}.

phase regions of the associated degenerate LG modes. As is evident, these phase elements are not radially symmetric so that the mode intensity patterns and corresponding losses cannot be calculated using matrix formulation, as previously described. It is possible, in principle, to resort to tensor formulation, but this considerably increases the complexity of the calculations. So, we will first consider the one-dimensional (1-D) *strip resonator* case [11], where the Hermite–Gaussian (HG) modes are selected with 1-D binary phase elements, in order to gain some insight. This insight, along with numerical Fox–Li calculations for the selected modes of lowest loss, will then be exploited to analyze our two-dimensional (2-D) resonator configuration.

In the case of a 1-D strip resonator, where the y-axis is infinite and the optical elements in Fig. 1 operate only on the x axis, the eigenvector $\boldsymbol{U_n}$ represents the field distribution along the x axis and is the same for all y's. The individual matrices in (3) are the same as before except for M_{FS}, which should be replaced either by the 1-D Fresnel propagator or, for short distances, by the 1-D angular spectrum propagator. The computed round-trip losses as a function of the aperture diameter, with and without a phase element for selecting the H_1 mode, are shown in Fig. 5. It is evident that the insertion of the phase element introduces considerable losses to the H_0 mode and has only a minor effect on the H_1 mode. To ensure that only the H_1 mode is selected the aperture diameter should be between 1.6–3.1 mm, depending on the laser resonator gain.

Similar behavior is expected in the case of the 2-D resonator configuration. The insertion of each of the phase elements depicted in Fig. 4 will have a minor effect on the selected mode, while introducing considerable losses to the undesired low order modes. In order to determine the relevant parameters for obtaining the optimal mode intensity distribution, round-trip loss, and beam quality M^2, when selecting a specific mode, we resort to numerical Fox–Li calculations. Specifically, we analyzed the 2-D resonator configuration shown in Fig. 1, using a commercial wave-simulation software[1] based on the Fox–Li iterative method with a fast Fourier transform propagation. Representative results are presented in Figs. 6–8. Fig. 6 shows the near- and far-field intensity distributions of the TEM_{00}, TEM_{01}, TEM_{02}, and TEM_{03} after inserting the appropriate binary phase elements. These results were obtained after 100 round-trip passes in the resonator starting from noise. Since the output beam acquires a uniform phase front, the far field distributions of the modes contain a bright central lobe with

[1]GLAD—Applied Optics Research.

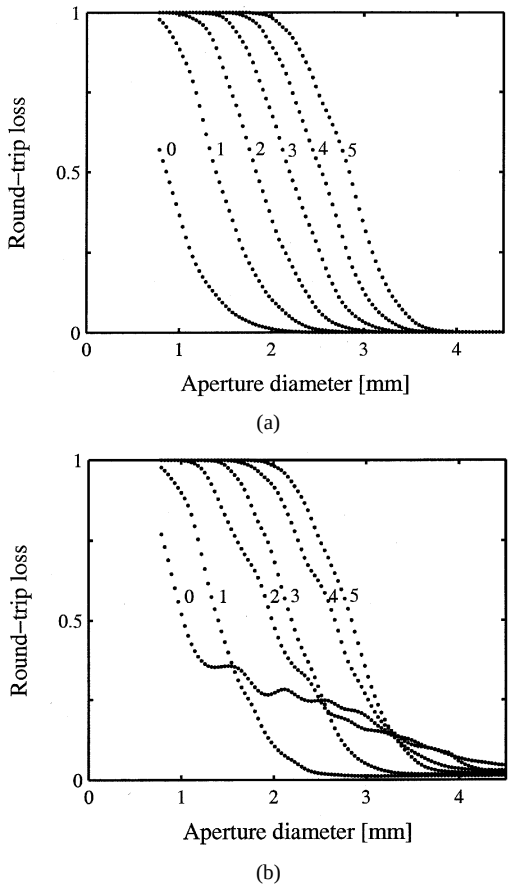

Fig. 5. Calculated round-trip losses of the lowest order HG modes for a one-dimensional resonator configuration. Resonator configuration geometry shown in Fig. 1. *Bare* configuration: (a) without phase element and (b) with phase element for selecting H_1 mode, placed 3.2 cm from the output coupler.

several low intensity side lobes. It is evident from Fig. 6 that mode selection is achieved in the examined configuration.

Fig. 7 shows the calculated (Fox–Li) round-trip loss for each of the selected modes at different aperture sizes. It should be noted that there is a range of suitable aperture diameters for the selection of a specific mode. Within this range, as the diameter decreases, the losses to the selected mode increase. On the other hand, a significant increase of the diameter is expected to result in multimode operation. It is of interest to note that the loss curves presented in Fig. 7 for the selected *degenerate* LG modes fit closely to the corresponding *nondegenerate* LG modes loss curves presented in Fig. 2. This can be explained by recalling that the degenerate LG mode is composed of two corresponding nondegenerate modes with opposite l signs (right and left helical phase fronts). Hence, the loss of the degenerate mode seems to be equivalent to the loss of the nondegenerate mode.

Finally, Fig. 8 shows the round-trip loss and the output beam quality parameter M^2 along the x direction as a function of the phase element position, when selecting the degenerate TEM_{01} mode. It can be seen that far from the output coupler, the round-trip loss increases rather linearly with the distance between the phase element and the output coupler. At short distances from the output coupler (less than 1 cm), the M^2 sharply increases along with a significant drop in the loss, indicating that the lowest loss mode is the TEM_{00} mode instead

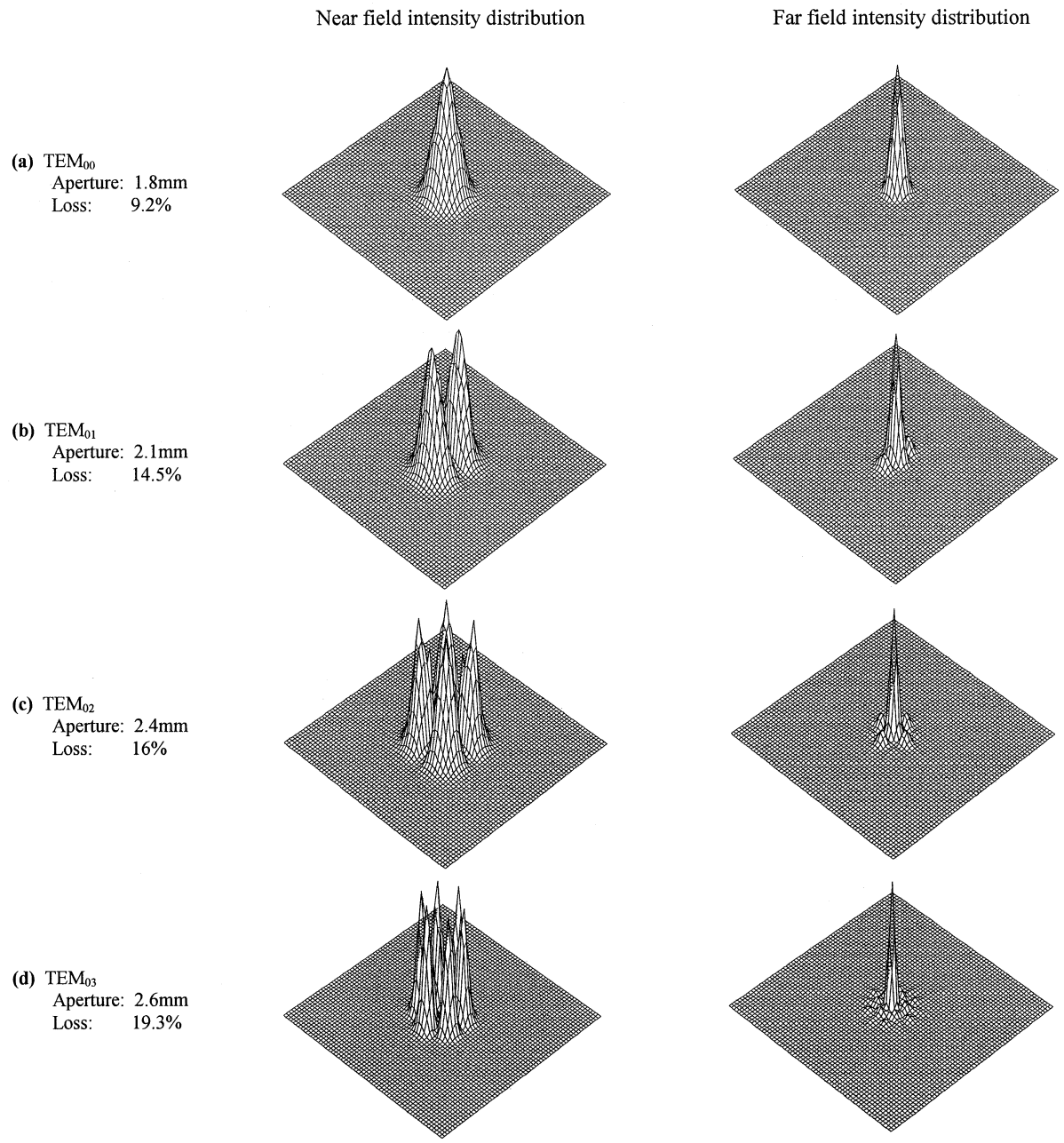

Fig. 6. Calculated results using Fox–Li iterative method when selecting specific LG modes with binary phase elements in the 2-D configuration. (a) TEM_{00} mode obtained without a phase element. (b) TEM_{01} mode obtained with the element in Fig. 4(a). (c) TEM_{02} mode obtained with the element in Fig. 4(b). (d) TEM_{03} mode obtained with the element in Fig. 4(c). The distance between the phase elements and the output coupler was 3.2 cm, numerical grid size was 256 × 256, grid spacing 2.5×10^{-5} m (for TEM_{03} 3.5×10^{-5} m), and the number of round trips, starting from noise, was 100.

of the TEM_{01} mode (the high M^2 originates from the π phase step the Gaussian beam acquires when exiting the resonator). As evident, good mode selection of the TEM_{01} is expected at distances of 1–5 cm from the output coupler.

The optimal aperture diameter and position of the phase element do eventually depend on the gain in the resonator and the difference between the loss curves of the selected mode and the next lowest loss mode (see, for example, Fig. 5). Generally, in the 2-D resonator configuration case, the next lowest loss mode could be determined by analyzing the beating of the two lowest-loss modes when applying the Fox–Li algorithm or alternatively by resorting to the Prony method [12].

III. Simple Model for Predicting the Relative Output Energies of the Selected Modes

We developed a simple model for predicting the expected relative output power (or energy) of each of the selected degenerate LG modes with radial order $p = 0$. In this model, we assume that the gain and the losses occur separately during each round-trip propagation in the resonator. In addition, we assume: 1) the modes are not greatly disturbed by the presence of the gain or by diffraction effects, and are nearly pure degenerate LG modes; 2) before introducing losses, or when the modes suffer equal losses, the peak intensity of each mode in the resonator

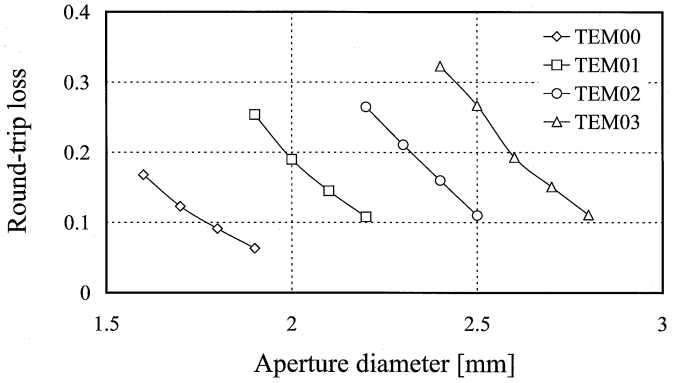

Fig. 7. Calculated Fox–Li round-trip losses as a function of the aperture size for the selected modes. Calculations were performed with the corresponding binary phase element located at a distance of 3.2 cm from the output coupler (except for the TEM_{00} mode where no phase element was used). The numerical grid size was 256 × 256, grid spacing 2.5×10^{-5} m (for TEM_{03} 3.5×10^{-5} m), and the number of round trips starting from noise was 100.

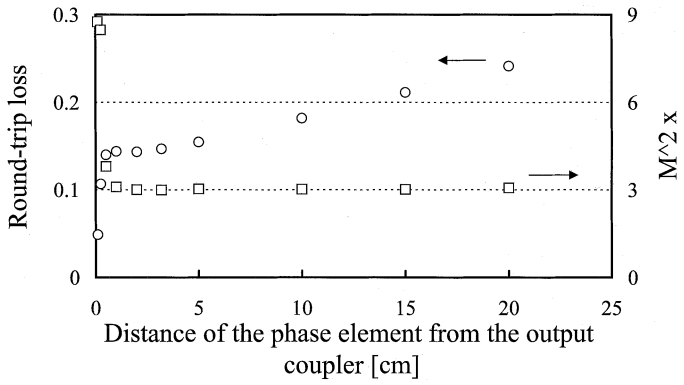

Fig. 8. Calculated Fox–Li round-trip loss (∘) and output beam quality M_x^2 (□) as a function of the distance between the phase element and the output coupler, for the degenerate TEM_{01} mode. The Numerical grid size was 256 × 256, grid spacing 2.5×10^{-5} m, and the number of round trips starting from noise was 100.

is the same. Detailed numerical analysis, based on equating the round-trip loss to the round-trip gain, taking into account the spatial profile of the modes, indicated that this latter assumption is reasonable.

Using the above assumptions, the intensity distributions of the degenerate LG modes inside the resonator are

$$I_{0,l}(\rho, \theta) = A\, l^{-l} e^{l} \rho^{l} e^{-\rho} \cos^2(l\theta) \qquad (5)$$
$$\text{with } \rho \equiv \frac{2r^2}{w^2}$$

where r and θ are the radial and azimuthal coordinates, respectively, l is the angular order of the mode, w is the *waist* or spot size of the lowest order Gaussian mode, and A is a normalization constant. The power contents of these modes, *assuming no losses*, are

$$P_{0,l}^{in} = A\, l^{-l} e^{l} \frac{\pi w^2}{2^k} \Gamma(l+1) \qquad (6)$$

where the value of k is 1 or 2, for $l = 0$ or $l > 0$, respectively, and the Gamma function Γ is defined as

$$\Gamma(n) = \int_0^\infty t^{n-1} e^{-t}\, dt; \qquad n > 0. \qquad (7)$$

Taking into account the diffraction losses γ_d in the specific mode-selecting configuration (depending on the aperture and position of the phase element), and output coupling losses γ_{oc}, the power of the beam at the output of the laser is then

$$P_{0,l}^{\text{out}} = (1-\gamma_d)(1-\gamma_{\text{oc}}) P_{0,l}^{in}. \qquad (8)$$

Recall that, for a specific mode-selecting configuration, the diffraction losses γ_d can be deduced from Fox–Li calculations (see Fig. 7).

Assuming equal diffraction losses, the relative power content of the TEM_{00}, TEM_{01}, TEM_{02} and TEM_{03} degenerate LG modes, calculated according to this simple model, is 1 : 1.36 : 1.85 : 2.23 respectively. It should be noted that in practical situations, where the diffraction losses for each selected mode are different, this power ratio would be altered (see for example Table I).

IV. Experimental Procedure and Results

In order to confirm our predictions, we performed a series of experiments using the experimental setup shown in Fig. 9. It includes the following:

1) a 71-cm-long plano-concave resonator, with a flat output coupler of 40% reflectivity at 1064 nm and a high reflective concave mirror with radius of curvature of 3 m;
2) a Nd : YAG rod of 5-mm diameter and 10-cm length, with 1.1% doping, placed in a diffusive ceramic pump chamber, and pumped at a constant level throughout the experiments.
3) A high-quality thin film polarizer (TFP).
4) A QS arrangement comprised of an electrooptical $LiNbO_3$ crystal and a $\lambda/4$ retardation plate. In QS operation, the pulsewidths were 20 ns (full-width at half maximum), while free-running operation was obtained by removing the retardation plate.
5) An aperture to limit the number of high order modes, positioned 22 cm from the output coupler.
6) CCD cameras and a Spiricon Laser Beam Analyzer, for detecting and characterizing the near- and far-field intensity distributions.
7) A phase element positioned a few centimeters from the output coupler.

Several binary phase elements for selecting TEM_{01}, TEM_{02}, and TEM_{03} degenerate LG modes were fabricated using photolithographic and reactive ion etching technologies to form the specific accurate depth profiles. These were subsequently coated with antireflection layers for 1064 nm using vacuum deposition technology. Representative actual profiles of midsections of two such elements, as measured with a ZYGO interferometer, are shown in Fig. 10. The measured surface roughness was in the range of 1–2 nm root-mean square (RMS).

Representative experimental results of the near and far field intensity distributions of light emerging from the QS laser, operating at a specific selected single mode, are presented in Fig. 11. For these results, the aperture diameter and the phase element position were optimized for the best performance.

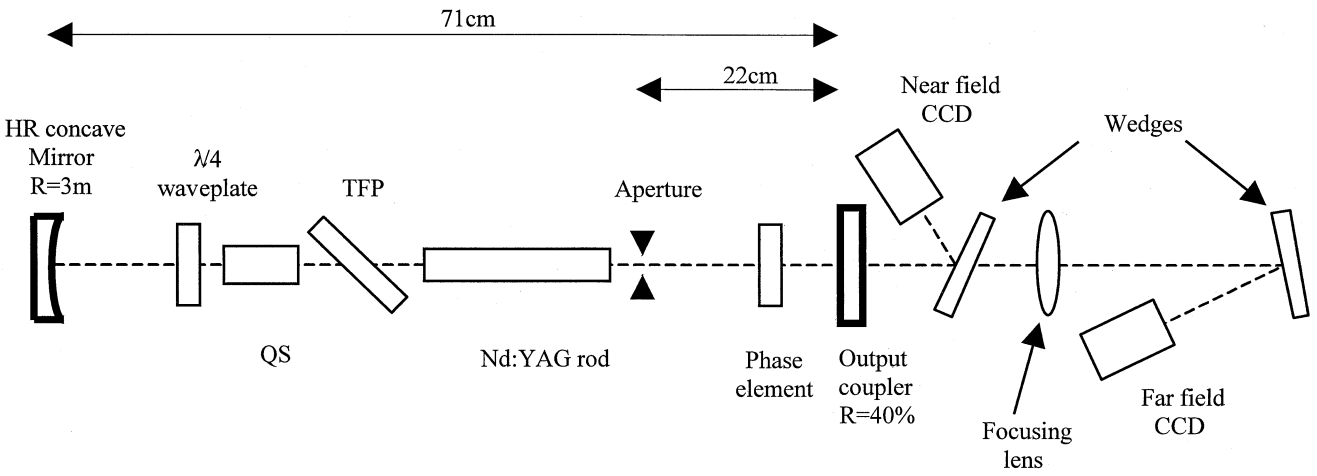

Fig. 9. Experimental Q-switched pulsed Nd : YAG laser setup for high-order mode selection.

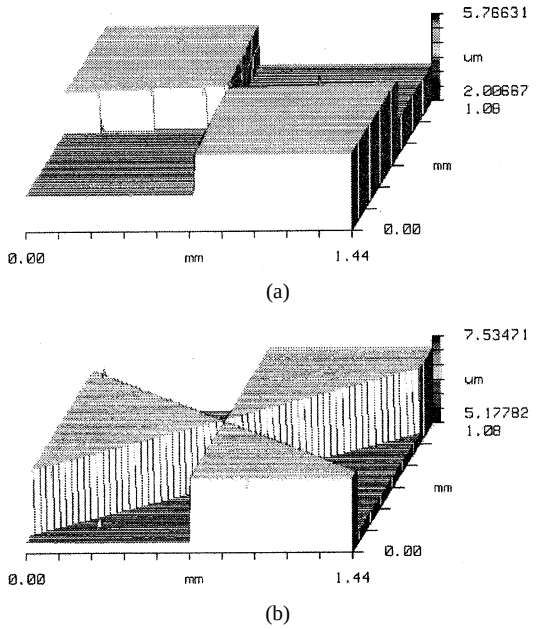

Fig. 10. Representative magnified interferometer (ZYGO) profile scans of two binary phase elements. (a) TEM_{02}. (b) TEM_{03}.

Specifically, the TEM_{00} was selected with an aperture diameter of 1.6 mm (without using any phase element). The TEM_{01} was selected with an aperture diameter of 2.1 mm and appropriate binary phase element positioned at a distance of 3.2 cm from the output coupler. The TEM_{02} was selected with aperture diameter of 2.2 mm and phase element position of 2.5 cm from the output coupler. Finally, the TEM_{03} was selected with an aperture diameter of 2.4 mm and phase element position of 2.5 cm from the output coupler. As evident, these experimental results are in good agreement with the calculated distributions shown in Fig. 6. The far-field distributions of the high-order modes consist of a high central peak surrounded by low side lobes, as expected. The experimental near field intensity distributions contain a low intensity ring-shaped pattern connecting the lobes. This pattern, which is not present with pure modes, seems to result from the phase element, which changes the phase of the mode to a uniform phase, before exiting the resonator. This phase uniformity accounts for the bright central peak in the far field, and also for the low-intensity ring-shaped patterns observed in the near field. This was verified experimentally by placing the phase element near the rear mirror instead of near the output coupler. In this case, the phase of the pure modes was not changed when exiting the resonator, so the near- and far-field intensity distributions were similar (as expected) and the ring patterns in the near field were not present.

We also measured the energies per pulse at the output of the laser when operating with each individual mode. The energy was 15 mJ with the TEM_{01} mode, 16.5 mJ with the TEM_{02} mode, and 18.3 mJ with the TEM_{03} mode, compared to an energy of only 10 mJ with the TEM_{00} mode. A comparison between the calculated and the measured relative output energies is presented in Table I. The calculated relative energies were obtained using the simple model described in Section III, taking the specific losses in each configuration from the data presented in Fig. 7. As is evident, the calculated results are in good agreement with the experimentally measured results.

In order to determine the effect of the increased losses that result from increasing the distance between the phase element and the output coupler, we measured the output energy as a function of the phase element position. The results for the degenerate TEM_{01} mode are presented in Fig. 12. As expected, the output energy is reduced as the phase element is positioned further away from the output coupler. We also found that the beam quality of the selected mode remains essentially constant at distances greater than 3.5 cm, as expected.

We investigated the behavior of the laser operating with a single high-order mode when it was Q-switched and when it was not. Representative results for a laser operating with the TEM_{02} mode are presented in Fig. 13. As is evident, the intensity distributions are very similar, although the pulse durations differed by almost four orders of magnitude, i.e., 20 ns in QS operation and 120 μs in non-QS operation. It should be noted that the optimal aperture diameter and the distance between the phase element and the output coupler were essentially the same in both cases. These results indicate that the high gain and short pulse duration seem to have only a minor effect in our laser configuration operating with a high-order mode.

Finally, we attempted to observe the mode evolution dynamics in QS operation by measuring the temporal pulse shape

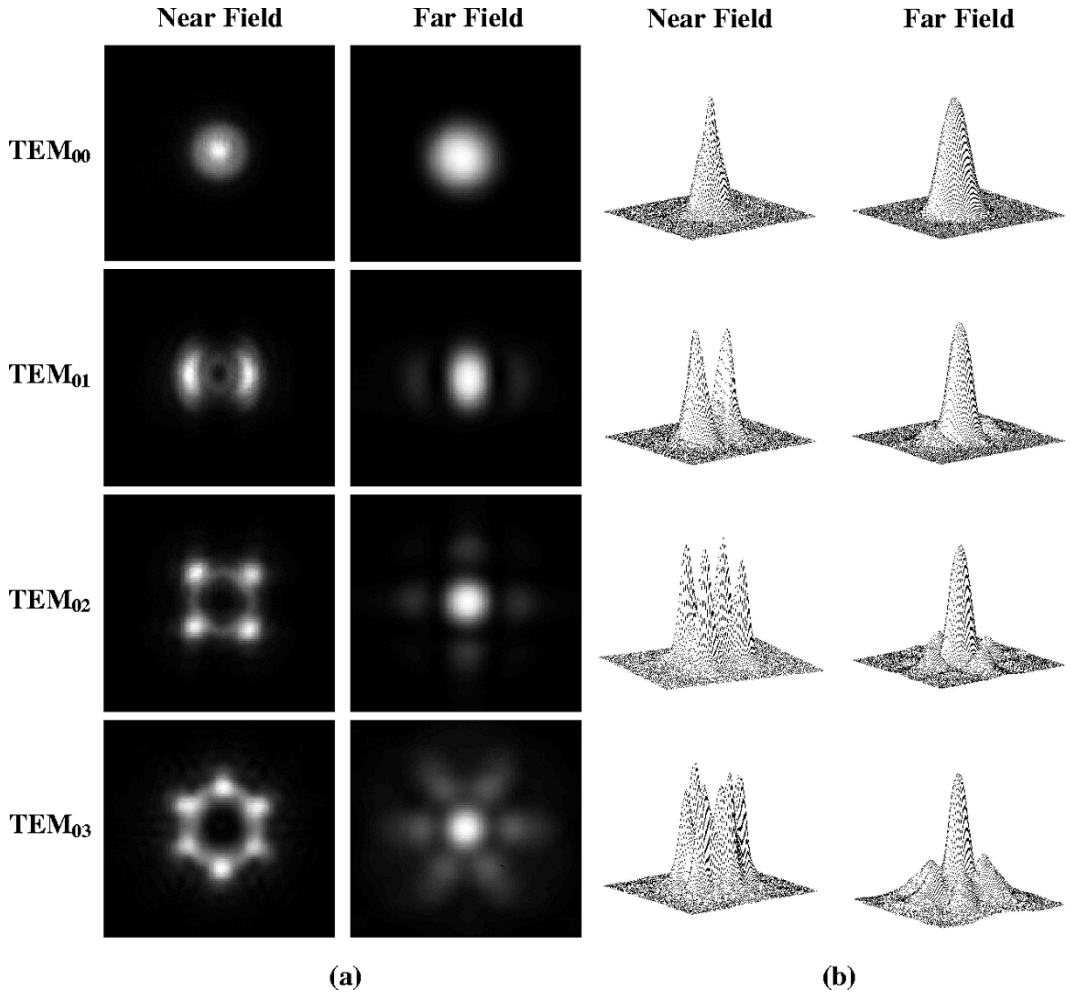

Fig. 11. Experimental near- and far-field intensity distributions of Nd:YAG Q-switched TEM_{00}, TEM_{01}, TEM_{02} and TEM_{03} LG modes. (a) Intensity distributions detected with a CCD camera. (b) Corresponding 3-D plots of the intensity distributions.

TABLE I
MEASURED AND CALCULATED RELATIVE OUTPUT ENERGIES OF THE SELECTED DEGENERATE LG MODES

Mode	Measured relative energy	Calculated relative energy
TEM_{00}	1	1
TEM_{01}	1.50	1.40
TEM_{02}	1.65	1.63
TEM_{03}	1.83	1.81

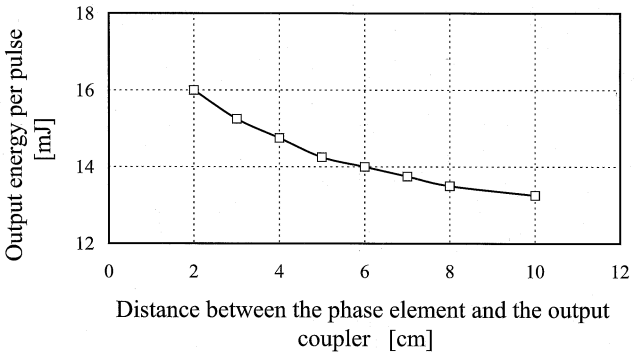

Fig. 12. Measured output energy of the TEM_{01} degenerate LG mode as a function of the distance between the phase element and the output coupler.

at various transverse locations in the output beam. We used a 0.2-mm aperture to measure the pulse shape in the low- and high-intensity regions of the output beam, and compared it with the average temporal pulse shape (integrated over the entire cross section of the beam). The experimental measurements for the laser operating with the degenerate TEM_{02} mode are presented in Fig. 14. As is evident, no significant change in the temporal pulse shape is observed. This result suggests good mode discrimination and rather fast mode buildup. It could be explained by an "early" evolution of the mode prior or during the opening of the QS, creating a very weak signal that seeds the large pulse which is formed when the QS opens completely.

V. CONCLUDING REMARKS

We successfully demonstrated efficient high-order mode selection in QS operation with the use of intra-cavity binary phase elements. A significant increase in the output energies relative to the fundamental TEM_{00} mode was achieved, and the optimized parameters for a specific laser configuration were determined. In order to obtain higher output energies, the ability to select higher transverse modes in high Fresnel number configurations should be further investigated. It should be noted that the

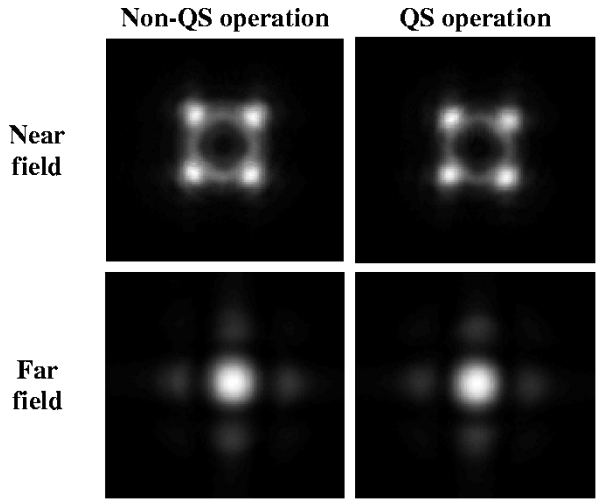

Fig. 13. Experimental near- and far-field intensity distributions of the degenerate TEM_{02} LG mode in non-QS and in QS operation.

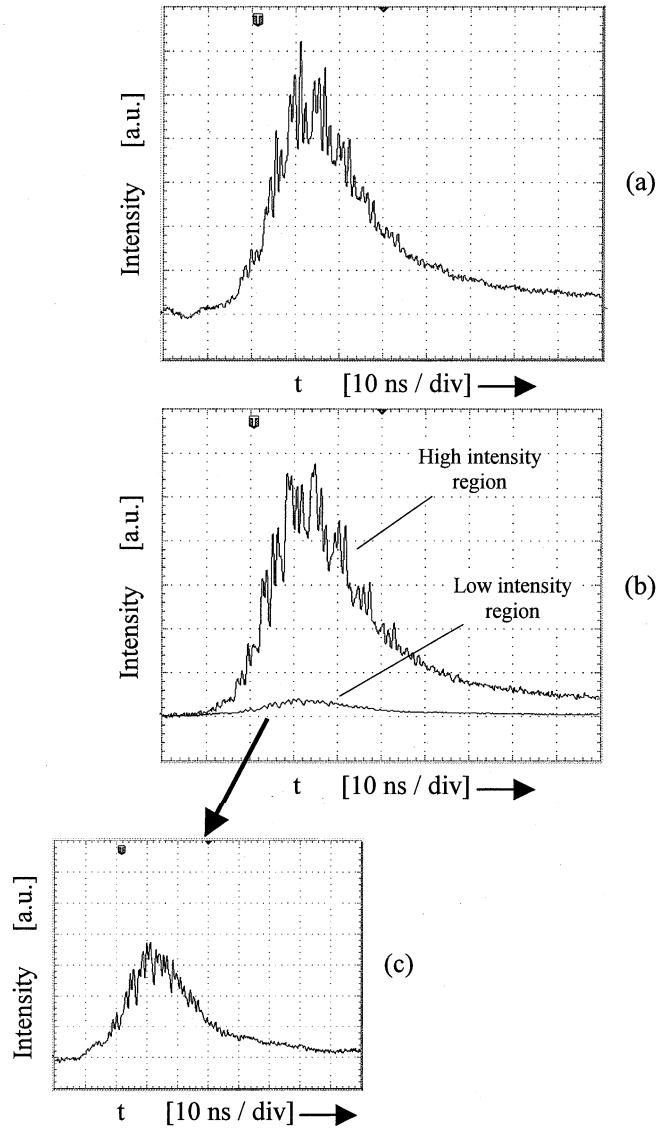

Fig. 14. Measured temporal pulse shape at the output of the laser operating with the TEM_{02} degenerate LG mode: (a) integrated over the whole pulse area in the near field; (b) through a 0.2-mm diameter aperture in the near field centered on one of the mode lobes (high intensity region) and near the center (low intensity region); and (c) detailed pulse-shape measurement through the aperture in the low-intensity region.

M^2 of the selected high-order modes is degraded relative to that of the fundamental TEM_{00} mode. However, since the entropy of a single high-order mode is equal to that of the fundamental mode, it is allowed thermodynamically to efficiently transform a single high order mode into a Gaussian beam, achieving excellent beam quality. Such a transformation can be performed externally by means of two specially designed phase elements [13], or by coherently adding various transverse parts of the mode [14].

Moreover, we introduced a simple model for predicting the relative output powers of the selected modes, which is in good agreement with the experimental results. Comparison of the mode selection in QS operation with that in non-QS operation, and preliminary investigation of the spatial evolution of the mode in QS operation, indicate that the high gain and short pulse duration seem to have only a minor effect in our laser configuration operating with a high-order mode.

REFERENCES

[1] R. Oron, N. Davidson, E. Hasman, and A. A. Friesem, "Transverse mode shaping and selection in laser resonators," *Progr. Opt.*, vol. 42, 2001.
[2] R. Oron, N. Davidson, A. A. Friesem, and E. Hasman, "Manipulating the Wigner distribution of high order laser modes," *Opt. Commun.*, vol. 193, pp. 227–232, 2001.
[3] ——, "Continuous phase elements can improve laser beam quality," *Opt. Lett.*, vol. 25, no. 13, pp. 939–941, 2000.
[4] R. Oron, Y. Danziger, N. Davidson, A. A. Friesem, and E. Hasman, "Discontinuous phase elements for transverse mode selection in laser resonators," *Appl. Phys. Lett.*, vol. 74, no. 10, pp. 1373–1375, 1999.
[5] ——, "Laser mode discrimination with intra-cavity spiral phase elements," *Opt. Commun.*, vol. 169, no. 1–6, pp. 115–121, 1999.
[6] A. Caprara and G. C. Reali, "Time varying M^2 in Q-switched lasers," *Opt. Quantum Electron.*, vol. 24, pp. S1001–S1009, 1992.
[7] A. E. Siegman, *Lasers*. Mill Valley, CA: Univ. Science Books, 1986, ch. 26.5, pp. 1034–1038.
[8] T. Li, "Diffraction loss and selection of modes in maser resonators with circular mirrors," *Bell Sys. Tech. J.*, vol. 44, pp. 917–932, 1965.
[9] D. Ehrlichmann, U. Habich, and H. D. Plum, "Azimuthal mode discrimination of annular resonators," *Appl. Opt.*, vol. 32, pp. 6582–6586, 1993.
[10] J. W. Goodman, *Introduction to Fourier Optics*, 2nd ed. New York: McGraw-Hill, 1996.
[11] A. G. Fox and T. Li, "Resonant modes in a maser interferometer," *Bell Sys. Tech. J.*, vol. 40, p. 453, 1961.
[12] A. E. Siegman, *Lasers*. Mill Valley, CA: University Science Books, 1986, ch. 14.3, p. 573.
[13] N. Davidson, A. A. Friesem, and E. Hasman, "Diffractive elements for annular laser beam transformation," *Appl. Phys. Lett.*, vol. 61, pp. 381–383, 1992.
[14] G. Machavariani, N. Davidson, A. A. Ishaaya, A. A. Friesem, and E. Hasman, "Efficient formation of a high-quality beam from a pure high-order Hermite–Gaussian mode," *Opt. Lett.*, vol. 27, no. 17, pp. 1501–1503, 2002.

Amiel A. Ishaaya (S'02) received the B.Sc. and M.Sc. degrees in physics from Tel Aviv University, Tel Aviv, Israel, in 1987 and 1995, respectively. He is currently working toward the Ph.D. degree at the Weizmann Institute of Science, Rehovot, Israel, focusing on high-order transverse mode selection in various laser configurations.

From 1986 to 1991, he served in the Israeli Defense Forces, conducting operations research and system analysis studies. From 1991 to 1994, he was with the Electrical Discharge and Plasma Laboratory, Tel Aviv University, Tel Aviv, Israel, performing research on cathode spot retrograde motion in high-current vacuum arc discharge systems. From 1994 to 2001, he was with ELOP—Electro-Optics Industries Ltd., Rehovot, Israel, working on military laser development projects. During this period, he specialized in the development of solid-state military lasers, and led several important projects.

Mr. Ishaaya is a member of the Optical Society of America.

Nir Davidson received the B.Sc. degree in physics and mathematics from the Hebrew University, Jerusalem, in 1982, the M.Sc. degree in physics from The Technion, Haifa, Israel, in 1988, and the Ph.D. in physics from the Weizmann Institute of Science, Rehovot, Israel, in 1992.

He was a post-doctoral Fellow at Stanford University, Stanford, CA, and is now a Senior Researcher in the Department of Physics of Complex Systems, at the Weizmann Institute of Science, Rehovot, Israel, where he holds the Rowland and Sylvia Schaefer Career Development Chair. His research is in the areas of laser cooling and trapping of atoms, precision spectroscopy, quantum optics, atom optics, Bose–Einstein condensation, and the field of physical optics. He has authored and co-authored over 100 journal and conference publications.

Dr. Davidson received the Allon Award for Senior Researchers for the Israeli Science Foundation, the Yosefa and Leonid Alshwang Prize for Physics from the Israeli Academy of Science, and the F. W. Bessel Award from the Humboldt Foundation. He is a member of the Optical Society of America, the American Physical Society, the Israeli Physical Society, and the Israeli Laser and Electro-Optics Society.

Galina Machavariani received the M.Sc. and Ph.D. degrees in physics from Rostov State University, Rostov-on-Done, Russia, in 1990 and 1995, respectively.

From 1989 to 1995, she was with Laboratory of Theoretical Physics, Rostov Institute of Physics, where her major fields of study were theory of core-level inelastic X-ray scattering in low-Z-atom crystals, resonance inelastic X-ray scattering spectra for low-symmetry crystals, and new approaches to the Green's function cluster calculations. From 1996 to 2001, she was with Tel-Aviv University, Tel-Aviv, Israel, as a post-doctoral Fellow, conducting investigations mainly in the area of phase transitions in solids at high pressures. In 2001, she joined Impala Advanced Laser Solutions Ltd., Rehovot, Israel. Her areas of research include diffractive optics, lasers, and phase elements for high-order mode selection in laser resonators. She has authored over 31 published papers.

Erez Hasman received the B.Sc. degree from the Tel Aviv University, Tel Aviv, Israel, in 1981, the M.Sc. degree from The Technion—Israel Institute of Technology, Haifa, in 1985, and the Ph.D. degree from Weizmann Institute of Science, Rehovot, Israel, in 1992.

During 1981–1986, he worked for the Department of Science, Government of Israel, Haifa, as a Senior Scientist. During 1992–1994, he was Chief Physicist of the graphic and recognition products line at Optrotech Company, performing research and development in the areas of photoploters and imaging systems for printed circuit boards and graphic arts industries. During 1994–1996, he was a Technology Analysis Manager at Elop Company, and a Scientific Consultant at Weizmann Institute of Science. During 1996–1998, he was a Senior Visiting Scientist at Weizmann Institute of Science and also a Scientific Consultant. Presently, he is an Associate Professor of Optical Sciences and Head of the Optical Engineering Laboratory, Faculty of Mechanical Engineering, The Technion—Israel Institute of Technology. His research is focused on subwavelength optical elements, diffractive optics, nano-optics, polarization state manipulations, optical metrology, optical storage, nonconventional laser resonators, and electro-optics devices.

Prof. Hasman is a member of the Optical Society of America and SPIE.

Asher A. Friesem (S'57–M'62–SM'79–F'95) received the B.Sc. and Ph.D. degrees from the University of Michigan, Ann Arbor, in 1958 and 1968, respectively.

From 1958 to 1963, he was with Bell Aero Systems Company, Buffalo, NY, and Bendix Research Laboratories, Southfield, MI. From 1963 to 1969, he was with the Institute of Science and Technology, University of Michigan, conducting investigations in coherent optics, mainly in the areas of optical data processing and holography. From 1969 to 1973, he was the Principal Research Engineer in the Electro-optics Center, Haris, Inc., Ann Arbor, MI, performing research in the areas of optical memories and displays. In 1973, he joined the staff of the Weizmann Institute of Science, Rehovot, Israel, becoming a Professor of Optical Sciences in 1977. His research includes new holographic concepts and applications, optical image processing, and electrooptics devices.

Dr. Friesem is the Vice President of the International Commission of Optics and Chairman of the Israel Laser and Electro-Optics Society. He is a Fellow of the Optical Society of America and a member of SPIE, Eta Kappa Nu, and Sigma Xi.